ELSEVIER

Chemical Geology 202 (2003) 5–21

CHEMICAL GEOLOGY
INCLUDING
ISOTOPE GEOSCIENCE

www.elsevier.com/locate/chemgeo

Origin of fluids and anhydrite precipitation in the sediment-hosted Grimsey hydrothermal field north of Iceland

T. Kuhn[a,*], P.M. Herzig[a], M.D Hannington[b], D. Garbe-Schönberg[c], P. Stoffers[c]

[a] *Department of Economic Geology, Leibniz Laboratory for Applied Marine Research, Freiberg University of Mining and Technology, Brennhausgasse 14, D-09596 Freiberg, Germany*

[b] *Geological Survey of Canada, 601 Booth Street, Ottawa, Canada K1A 0E8*

[c] *University of Kiel, Institute of Geosciences, Olshausenstr. 40, D-24118 Kiel, Germany*

Received 8 February 2002; accepted 4 June 2003

Abstract

The sediment-hosted Grimsey hydrothermal field is situated in the Tjörnes fracture zone (TFZ) which represents the transition from northern Iceland to the southern Kolbeinsey Ridge. The TFZ is characterized by a ridge jump of 75 km causing widespread extension of the oceanic crust in this area. Hydrothermal activity occurs in the Grimsey field in a 300 m × 1000 m large area at a water depth of 400 m. Active and inactive anhydrite chimneys up to 3 meters high and hydrothermal anhydrite mounds are typical for this field. Clear, metal-depleted, up to 250 °C hydrothermal fluids are venting from the active chimneys. Anhydrite samples collected from the Grimsey field average 21.6 wt.% Ca, 1475 ppm Sr and 3.47 wt.% Mg. The average molar Sr/Ca ratio is 3.3×10^{-3}. Sulfur isotopes of anhydrite have typical seawater values of 22 ± 0.7 ‰ $\delta^{34}S$, indicating a seawater source for SO_4^{2-}. Strontium isotopic ratios average 0.70662 ± 0.00033, suggesting the precipitation of anhydrite from a hydrothermal fluid–seawater mixture. The endmember of the venting hydrothermal fluids calculated on a Mg-zero basis contains 59.8 μmol/kg Sr, 13.2 mmol/kg Ca and a $^{87}Sr/^{86}Sr$ ratio of 0.70634. The average Sr/Ca partition coefficient between the hydrothermal fluids and anhydrite of about 0.67 implies precipitation from a non-evolved fluid. A model for fluid evolution in the Grimsey hydrothermal field suggests mixing of upwelling hydrothermal fluids with shallowly circulating seawater. Before and during mixing, seawater is heated to 200–250 °C which causes anhydrite precipitation and probably the formation of an anhydrite-rich zone beneath the seafloor.

Keywords: Seafloor hydrothermal system; Anhydrite; Sr isotopes; Tjörnes fracture zone; Grimsey; Iceland

1. Introduction

Iceland is one of the most active volcanic regions on Earth. It is dominated by the subaerial expression of the Mid-Atlantic Ridge where it crosses the Iceland hotspot. The axial rift zone on Iceland is made up of a number of volcanic centres (i.e., Krafla and Vatnajokull volcanoes). To the south it is continuous with the Reykjanes Ridge offshore (Fig. 1). To the north there is no obvious offshore expression of the ridge, and the link between the Kolbeinsey Ridge and the neovolcanic zone is characterized by a 75-km-wide oblique

* Corresponding author. Fax: +49-3731-39-2610.
E-mail address: Thomas.Kuhn@mineral.tu-freiberg.de (T. Kuhn).

0009-2541
doi:10.1016/S0009-2541(03)00207-9

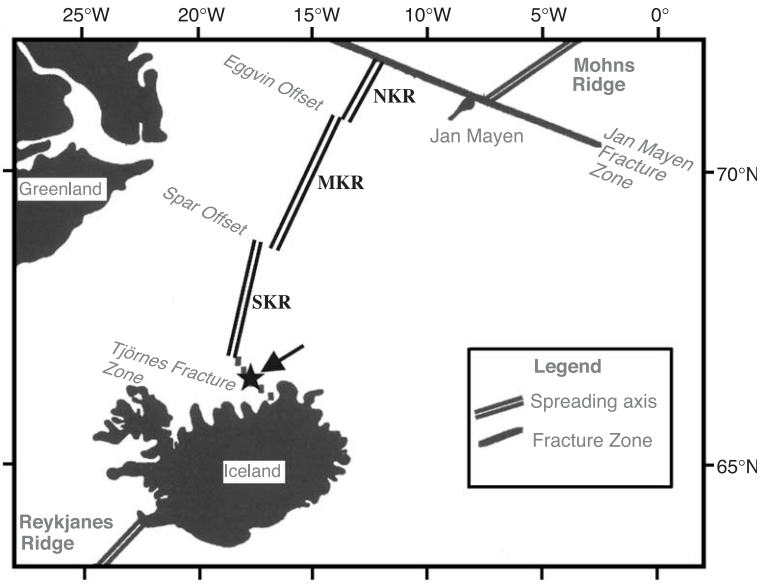

Fig. 1. The position of the Grimsey hydrothermal field (GHF) within the Tjörnes FZ which is an oblique extensional zone linking Iceland with the southern Kolbeinsey Ridge (SKR; from Devey et al., 1997).

extensional zone known as the Tjörnes fracture zone (TFZ, Fig. 1; Rögnvaldsson et al., 1998).

Submarine hydrothermal activity around Iceland is known from the Kolbeinsey and Reykjanes Ridges (German et al., 1994; Olafsson et al., 1989) and shallow-water hot springs are known where land-based geothermal systems continue offshore (Benjaminsson, 1988). However, before the late 1980s, hydrothermal activity within the TFZ was only known from gas bubbles observed by fishermen just south of Kolbeinsey Island and by hydrothermal material occasionally recovered in fishing nets. A cruise of R/V *Polarstern* in 1988 using the manned submersible *Geo* eventually discovered hydrothermal venting at the seafloor within the TFZ (Fricke et al., 1989). During two cruises of R/V *Poseidon* (PO 229, 1997 and PO 253, 1999), hydrothermal activity was located at three locations: south of Kolbeinsey Island, east of Grimsey Island and in Akureyri Bay (Stoffers et al., 1997; Scholten et al., 2000; Hannington et al., 2001). The most intense hydrothermal activity was found at the sediment-hosted Grimsey field, which is a 300 m × 1000 m large area hosting numerous actively venting anhydrite chimneys on coalesced anhydrite mounds. At 400 m water depth, the 250 °C clear fluids show signs of subcritical phase separation (boiling). Hannington et al. (2001) suggested that the active Grimsey field is underlain by a large boiling zone and that sulfide precipitation at depth could explain the strong metal depletion of the venting fluids.

In this paper we discuss Sr and S isotopic ratios, element geochemistry and fluid inclusion data of anhydrite and hydrothermal fluids sampled with the research submersible *Jago* during cruise PO 229 of R/V *Poseidon* (Stoffers et al., 1997). Anhydrite in hydrothermal systems forms from mixing of hydrothermal fluids with seawater which entrains the seafloor. This mixing is recorded in the Sr isotopic composition of fluids or minerals (Mills and Tivey, 1999). Such data coupled with Sr/Ca ratios of fluids and anhydrites allow the reconstruction of fluid evolution at depth. In turn, changes in the composition of hydrothermal fluids have further consequences on the precipitation of other minerals. Since anhydrite has a retrograde solubility (it is stable between ~ 150 and ~ 250 °C), precipitation and dissolution of anhydrite through time also has the potential to modify the structure of a hydrothermal deposit. This is not only important for modern seafloor deposits but has implications for fossil on-land analogues (Mills and Tivey, 1999).

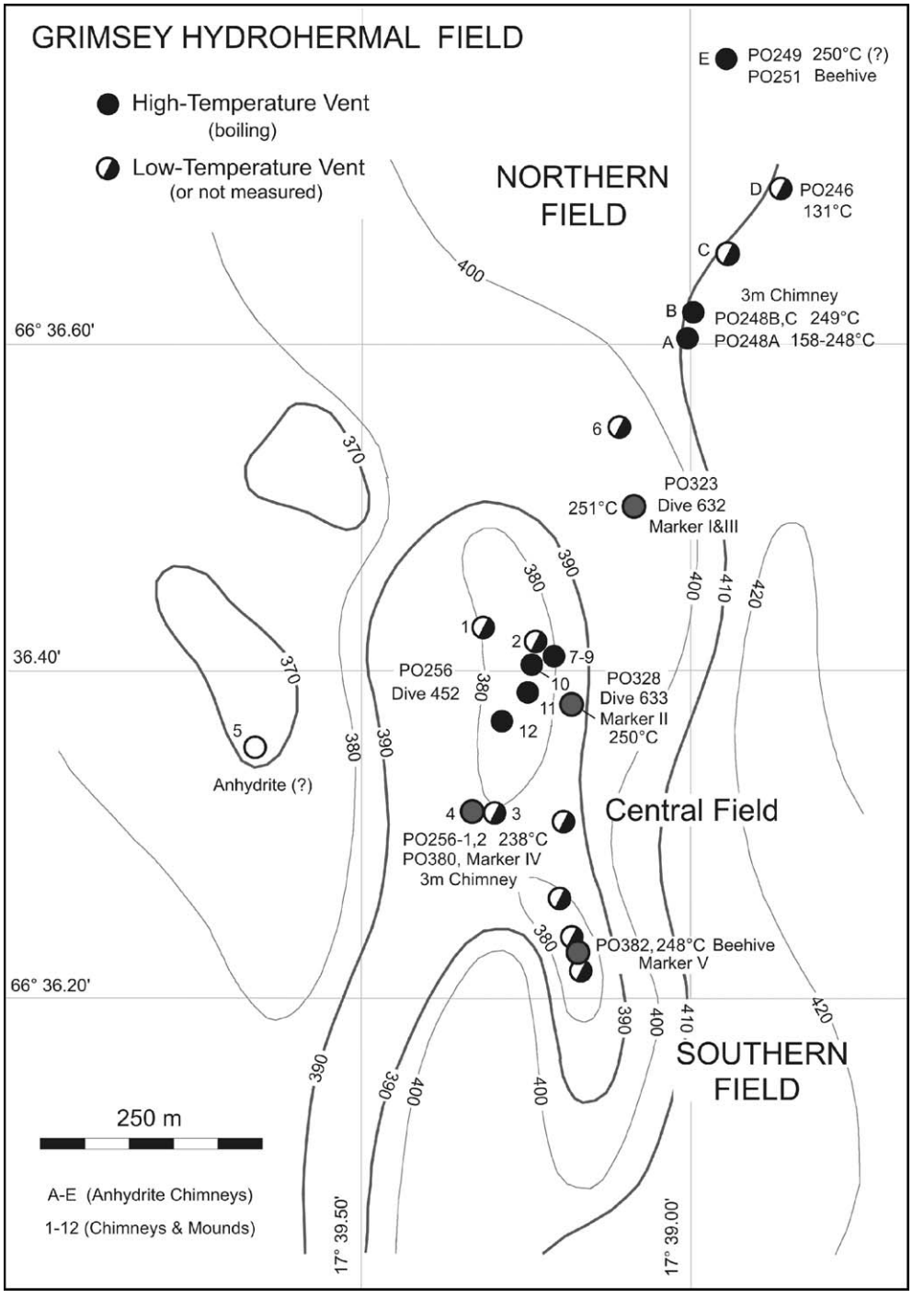

Fig. 2. Bathymetry of the Grimsey hydrothermal field with the location of vent sites, sampling sites (see also Table 1) and in situ temperatures of the emanating fluids (from Scholten et al., 2000).

Despite the importance of anhydrite, there are only a few systematic studies of this mineral in hydrothermal systems (e.g., Shikazono et al., 1983; Mills et al., 1998; Teagle et al., 1998a,b; Mills and Tivey, 1999). The widespread occurrence of massive anhydrite in mounds and chimneys of the Grimsey field provides a substantial sample basis for a systematic study of this important mineral. The Grimsey hydrothermal field is especially important since it provides the first occurrence of massive anhydrite in shallow water depth.

2. Analytical methods

After subsampling of anhydrite chimneys, XRD analyses were carried out to investigate the mineralogical composition of the samples. They were ground to <62 μm and scanned from 5° to 80° 2θ using a RD7 with Cu tube at the XRD laboratory of Freiberg University. Qualitative phase-analysis of the diffraction patterns was carried out by conventional search/match procedures using reference diffraction patterns stored in the ICDD PDF-2 (International Centre for Diffraction Data).

Anhydrite samples were then analyzed by AAS after total digestion of a 100-mg sample with HF/HNO_3 to determine concentrations of Ca, Mg and Sr. The Ca content was analyzed using a titration method if Ca>20 wt.%. After HF/HNO_3 digestion, the solution was titrated against m/20 EDTA using Fluorexon as indicator. For a description of both methods, see Heinrichs and Herrmann (1990). The analyses were carried out at the Geochemical Laboratories of Freiberg University. Analytical precision was checked against in-house standards and was generally better than 2%.

Hydrothermal fluids were sampled with 5 l Niskin bottles mounted on a frame at the front end of the submersible *Jago*. Immediately after recovery of the submersible, fluid samples were collected in prewashed and N_2 purged 1 l FEP Teflon bottles for

Table 1
Sample description and location

Station	Location	Depth (m)	Sample	Description
PO 246	East Grimsey (North)	406–402	PO 246-A-1	from small, intact chimney (25–30 cm) with dark grey needle-shaped anhydrite on outer crust and colloform anhydrite in central conduit (*T* of venting fluid when chimney was knocked over: 130 °C)
		410–402	PO 248-A-3	miscellaneous pieces from anhydrite chimney which vented 158 °C hot fluid; 249 °C when chimney was knocked over (0.5–1 kg total)
			PO 248B	*B-2:* large, hard, massive anhydrite piece from central conduit of chimney that was knocked over (2-cm-thick massive anhydrite wall; 0.5 cm inner zone of crystalline anhydrite coated in pale yellow material; 0.5 cm outer zone of grey, dirty anhydrite) *B-3:* two pieces of small (10 cm) delicate, thin-walled anhydrite chimneys; more massive colloform anhydrite at base
PO 249	East Grimsey (North)	403	PO 249	small crust of massive anhydrite (0.5 kg), 0.5 m from beehive chimney at north end of field
PO 251	East Grimsey (North)	402	PO 251	intact chimney (0.4 m tall) adjacent to 250 °C vent (beehive) at northern end of field *251-1:* large chimney piece (35 cm), dark stained anhydrite on outer rim and massive porous anhydrite in central conduit *251-2:* smaller chimney (20 cm), 2 cm walls, 3 cm central conduit, pale yellow precipitate in interior (as in 248-B-2) *251-3:* 3 kg of massive anhydrite with grey precipitate (stained anhydrite) lining the central conduit of chimney fragments
PO 256	East Grimsey (Central)	383	PO 256	small, 1-m-high, 2-m-wide anhydrite chimney on top of low mound *256-2:* base of boiling chimney (238 °C) after it was knocked over, 2–3 cm thick anhydrite wall, grey, smoky anhydrite on exterior; distinctive pink to yellow precipitate lining interior

subsequent filtration and sample preparation. Any contact of the water sample with ambient air was avoided. Samples for Sr, Ca and Mg contents as well as for Sr isotopes were then pressure-filtrated through 0.4 μm polycarbonate membrane filters (Nuclepore) using nitrogen 5.0 and subsequently acidified with five drops subboiled hydrochloric acid. Magnesium and Ca were analyzed by ICP-AES, Sr concentration was determined by ICP-MS at the University of Kiel. International seawater standards CASS-3, NASS-4 and SLRS-3 as well as sample duplicates and procedural blanks were used for analytical quality control.

Sulfur isotope analyses of anhydrite were carried out using a Finnigan MAT Delta E mass spectrometer. Samples were decomposed and oxygenated using V_2O_5–quartz mixtures according to the method of Ueda and Krouse (1986). Accuracy of the analyses was checked against the international standards NBS-127 (published value: 20.3‰ $\delta^{34}S$; measured value of five duplicates: 20.64 ± 0.24‰ $\delta^{34}S$) and IAEA NZ1 (published value: -0.30‰ $\delta^{34}S$; measured value of five duplicates: -0.26 ± 0.10‰ $\delta^{34}S$). The reproducibility was generally better than ± 0.2‰ $\delta^{34}S$. All data are reported relative to the Canyon Diablo Troilite (CDT).

The $^{87}Sr/^{86}Sr$ ratios of anhydrite, least-altered sediments and fluid samples were measured with a Finnigan MAT 262 mass spectrometer. The anhydrite samples were digested in 2.5 N HCl, the sediments were digested in concentrated HNO_3–HF (1:5), vaporized and again digested in 2.5 N HCl; the fluid samples were vaporized and digested in 2.5 N HCl. Finally all samples were eluated to $SrCl_2$, vaporized and condensed in deionized water and eventually fixed with H_3PO_4 on Ta filaments. Accuracy of the analyses was checked against the international standard NBS-987 (published value: 0.71025 $^{87}Sr/^{86}Sr$; measured value of six duplicates: 0.71024 ± 0.000074 $^{87}Sr/^{86}Sr$; cf. Tichomirowa et al., 2001).

Table 2
Sr isotopic data and selected trace element geochemistry of hydrothermal fluids from the Grimsey field compared to literature data

Sample ID	Temperature (°C)[a]	$^{87}Sr/^{86}Sr \pm 2s$	Sr (μM)	Ca (mM)	Mg (mM)	Sr/Ca (mmol/mol)	Proportion of hydrothermal component (%)[b]
Grimsey field							
248-1	249	0.709094 ± 0.000053	84.2	9.56	47.6	8.81	6 (9)
248-2	250	0.709121 ± 0.000041	84.7	9.61	47.2	8.81	5 (7)
249-1	250	0.708827 ± 0.000033	83.6	9.86	42.8	8.48	19
249-2	250	0.708469 ± 0.000021	78.9	10.3	36.9	7.66	34
251-1	248	0.708565 ± 0.000040	80.8	10.4	39.1	7.77	31
251-2	248	0.709022 ± 0.000022	85.5	9.71	46.5	8.81	10
Mean		0.708850 ± 0.00035	83	9.91	43.4	8.39	24
Std.			3	0.36	4.53	0.54	11.1
Endmember based on Mg = 0		0.70634	59.8	13.2		4.53	
Seawater—this study	2.6	0.709225 ± 0.000032	88.6	9.33	53.1	9.50	
Middle Valley, AAV site[c]	180–275	0.7042	257	81		3.17	
Escanaba Trough[c]	108–217	0.7099	209	33.4		6.25	
Guaymas Basin, South Field[c]	250–308	0.7059	158	27.7		5.7	
TAG, white smoker fluid[d]	273–301	0.70319	91	27		2.62	
MARK'86[d]	335–350	0.7028	50	10		5	

Data for c and d from Mills et al. (1998); Goodfellow and Zierenberg (1999).

[a] Fluid temperature measured with a *T* probe at the discharge sites.

[b] Relative proportion of hydrothermal component in venting fluids which was calculated according to Mills et al. (1998). Values in parantheses for samples 248 are calculated taking the maximum analytical error into account.

[c] Sediment-covered (AAV = Area of Active Venting).

[d] Sediment-free.

Microthermometric studies of anhydrite were carried out on doubly polished thick sections using a USGS gas-flow heating–freezing stage. A three-point calibration at −55.6, 0 and 374.1 °C was conducted with an accuracy of ±1 °C between −60 and +100 °C. The homogenization temperatures were measured according to the cyclus method in 5 °C/min steps up to 150 °C. When homogenization was approached, the heating intervals were changed to 1 °C/min. Salinities were determined from freezing experiments and calculated according to the equation given by Bodnar (1993) assuming a pure NaCl–H_2O system. Therefore, all results are given in wt.% NaCl equivalent.

3. Results

3.1. Sample origin

Samples collected for this study are from the central and northern areas of the Grimsey hydrothermal field (Fig. 2). These areas consist of isolated mounds and solitary chimneys (northern field) and large coalesced anhydrite mounds and chimneys (central field). There is also a smaller southern field of old but still active mounds. The mounds are large-diameter, low-relief structures up to 10 m across and 3–5 m high. They are capped by numerous 1–3 m tall anhydrite-rich spires

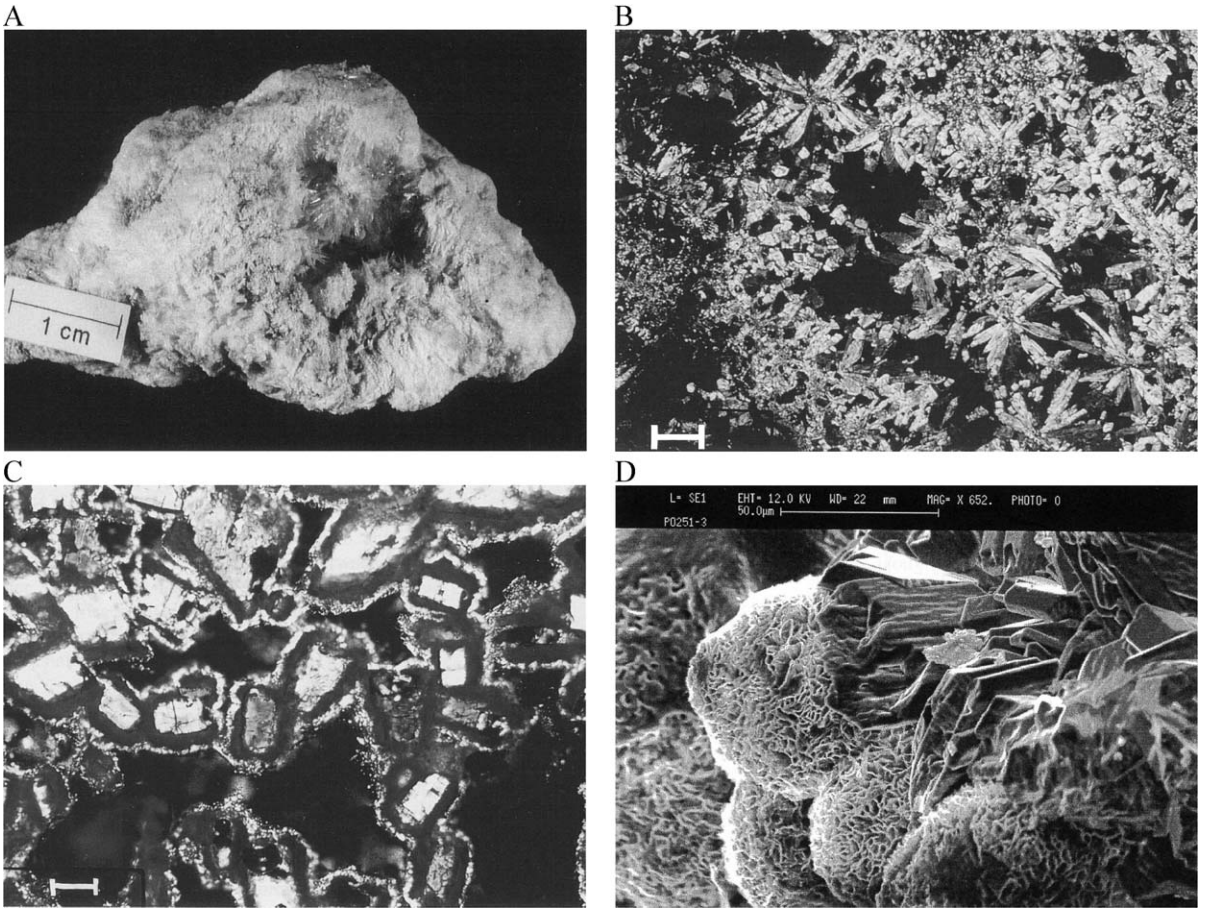

Fig. 3. (A) Massive and acicular anhydrite from a beehive-structured chimney (sample PO 251-3). (B) Photomicrograph of anhydrite from an active chimney showing radially fibrous crystals and (C) rectangular crystals (measure in B and C: 400 µm; crossed Nicols, sample PO 248-B-2). (D) A spongy talc-like material grows on top of euhedral anhydrite (SEM of sample PO 251-3). All samples are from active chimneys (fluid temperatures about 250 °C). For sample location, see Fig. 2.

with pinkish brown to pale yellow, talc-like material lining the inner fluid channelways (Hannington et al., 2001). The chimneys have a thick wall, up to 20 cm in width, composed of dense, hard anhydrite (Table 1). The hydrothermal mounds consist of anhydrite, gypsum, terrigenous and hydrothermal clay, and talc-like material. In the main field, the mounds coalesce to a 300-m-long and 1000-m-wide ridge. From gravity cores it is known that anhydrite shows some post-burial dissolution and recrystallization effects. Pyrite and marcasite were found locally as encrustations in fluid channels in the sediments and as massive, rusty crusts (at location of Marker IV, Fig. 2). However, other sulfides were not found on the seafloor or in 3-m-long sediment cores.

3.2. Hydrothermal fluid geochemistry

Hydrothermal fluids are venting from most of the chimneys as well as through fissures and cracks from the surrounding seafloor. The clear, metal-depleted fluids reach temperatures up to 250 °C (Fig. 2; Table 2) and typically show effects of phase separation (see Discussion section; Hannington et al., 2001). Their endmember Ca and Sr concentrations are rather low compared to other sediment-hosted hydrothermal systems, but similar to sediment-free, MORB-hosted systems like TAG or MARK (Table 2). The molar Sr/Ca ratio is within the variation of sediment-hosted hydrothermal systems and it is about half the value of seawater.

3.3. Petrography and element geochemistry

At the Grimsey field, pure anhydrite, anhydrite intergrown with gypsum, talc-like phases and minor amounts of sulfides were sampled (Table 1). Anhydrite exhibits a variety of habits from fine to coarse grained, cauliform, acicular, and radially fibrous to euhedral grains (Fig. 3A–C). Sulfides at the Grimsey field form small subhedral to euhedral pyrite grains of about 5 μm in size, partly embedded in amorphous silica (Stegmann, 1998). SEM analyses show hydrothermal talc-like material (kerolite–stevensite?) grown onto euhedral anhydrite (Fig. 3D).

XRD analyses show that most of the samples of this study consist of rather pure anhydrite (Table 3). The most common accessory mineral is gypsum which mainly occurs in traces, except for samples PO 251-1/-2 and PO 256-2. The latter sample also contains a high amount of a stevensite–kerolite mixed layer. Stevensite is a smectite and kerolite is a partly disordered talc. No other minerals (e.g., barite, amorphous silica or quartz) occur in the samples.

Table 3
Results of X-ray diffraction analyses on anhydrite samples of this study

Sample ID	Anhydrite	Gypsum	Talc-like (kerolite–stevensite)
PO 246-A-1	xxx	o	
PO 246-C	xxx	x	
PO 248-A-3	xxx	o	
PO 248-B-2	xxx	x	
PO 248-B-3	xxx		
PO 249	xxx	o	o
PO 251-1	xxx	xx	o
PO 251-2	xx	xx	
PO 251-3	xxx	x	x
PO 256-2	xxx	xx	xxx

o: traces; x: minor, xx: common, xxx: abundant.

Analytical results of anhydrite-rich samples are presented in Table 4. Strontium concentrations vary between 1028 and 1953 ppm, Ca in the bulk sample between 8.37 and 28.7 wt.%. The rather high Mg contents of samples PO 248-B-2, PO 249 and PO 256-2 are caused by admixture of talc-like material (kerolite–stevensite mixed layer) which is even dominant in sample PO 256-2 (Table 3). Such talc-like phases can precipitate from seawater-hydrothermal mixtures at high temperatures (>240 °C; Bischoff and Seyfried, 1978) and occur submicroscopically in black smoker chimneys from the East Pacific Rise (EPR; Haymon and Kastner, 1986). The correlation coefficient is 0.777 between Sr and Ca reflecting the substitution of Ca by Sr in the anhydrite lattice due to their similar cationic radius (Sr^{2+} = 1.26 Å; Ca^{2+} = 1.12 Å; Shannon, 1976). Strontium contents are very similar to anhydrites from the Area of Active Venting in the sediment-covered hydrothermal Middle Valley system (Goodfellow and Zierenberg, 1999); however, they are clearly lower than anhydrite precipitated in a black smoker chimney from 21°N EPR. By comparison, Sr contents of anhydrite sampled from some ancient massive sulfide deposits are rather low relative to modern seafloor hydrothermal vents (Table 4).

Table 4
Sr isotopic data and selected trace element geochemistry of anhydrites from the Grimsey hydrothermal field compared to literature data

Sample ID	$^{87}Sr/^{86}Sr \pm 2s$ anhydrite	Sr (ppm)	Ca (%)	Mg (%)	Sr/Ca (mmol/mol)	Partition coefficient D_{Sr}[a]
Grimsey field						
PO 246-A-1	0.70662 ± 0.000035	1696	23.10	3.38	3.35	0.74
PO 246-C	0.706763 ± 0.000026	1302	26.59	0.77	2.24	0.49
PO 248-A-3	0.706236 ± 0.000017	1915	28.20	0.33	3.10	0.68
PO 248-B-2	0.706081 ± 0.000044	1220	18.40	5.75	3.03	0.67
PO 248-B-3	0.706188 ± 0.000047	1953	28.70	0.35	3.11	0.69
PO 249	0.707319 ± 0.000030	1047	14.51	5.54	3.30	0.73
PO 251-1	0.706665 ± 0.000025	1813	23.70	1.98	3.49	0.77
PO 251-2	0.706354 ± 0.000031	1635	22.20	2.67	3.36	0.74
PO 251-3	0.706312 ± 0.000043	1140	22.03	1.18	2.36	0.52
PO 256-2	0.707625 ± 0.000032	1028	8.37	12.79	5.61	1.24
Mean	0.706616 ± 0.000033	1475	21.58	3.47	3.30	0.67[b]
Std.		365	6.34	3.82	0.92	0.10[b]
PO 253/SL339[c]	0.704512 ± 0.00034	240	4.95	2.88	2.22	
TAG ($n=21$)	0.704512 ± 0.000010[d]	2141[d]	29.44[d]	0.02[d]	3.33[d]	0.53–3.5[e]
Middle Valley						
AAV ($n=6$)	0.70655	1583	27.1	1.68	2.68	
21°N EPR ($n=2$)		3418	26.1		5.99	
Fossil Kuroko						
Deposits ($n=15$)	0.70781 ± 0.00005	482				

Middle Valley: anhydrite chimneys of area of active venting (AAV): Ames et al. (1993); Sr isotopes: 1 gypsum analysis: Goodfellow et al. (1993).
Kuroko: anhydrites from massive sulfides and late veins; Shikazono et al. (1983).
EPR: anhydrite from a black smoker; Haymon and Kastner (1981).
[a] Using Sr/Ca of endmember hydrothermal fluid (=4.53)—this study.
[b] Without PO 256-2 because of high stevensite–kerolite contamination.
[c] Least-altered sediments from the Grimsey field area.
[d] From Teagle et al. (1998a).
[e] Calculated values for TAG anhydrites suggesting an evolving black smoker fluid–seawater mixture (Mills and Tivey, 1999).

Molar Sr/Ca ratios do not vary appreciably, except in the Mg-rich sample PO 256-2. They are similar to measured values from TAG anhydrites and lower than values from EPR black smoker anhydrite, but higher than the Middle Valley samples (Ames et al., 1993; Teagle et al., 1998a; Table 4). Moreover, molar Sr/Ca ratios are distinctly lower than seawater (Table 2).

3.4. Isotope geochemistry

Sulfur isotopic ratios of anhydrites from the Grimsey field range between 21.2‰ and 22.7‰ with a mean of 22.0‰ $\delta^{34}S$ ($n=10$; Table 5). These ratios are somewhat higher than seawater and typical 21°N

Table 5
Sulfur isotope ratios of anhydrites from Grimsey field

Sample ID	Description	$\delta^{34}S_{CDT}$[‰]
PO 246-A-1	anhydrite, gypsum	22.4 ± 0.2
PO 246-C	anhydrite, gypsum	21.6 ± 0.2
PO 248-A-3	anhydrite, gypsum	21.2 ± 0.2
PO 248-B-2	anhydrite, gypsum	21.8 ± 0.2
PO 248-B-3	anhydrite	21.6 ± 0.2
PO 249	anhydrite, gypsum, stevensite	22.1 ± 0.2
PO 251-1	anhydrite, gypsum, stevensite	22.6 ± 0.2
PO 251-2	anhydrite, gypsum	22.7 ± 0.2
PO 251-3	anhydrite, gypsum	21.2 ± 0.2
PO 256-2	anhydrite, stevensite, gypsum	22.7 ± 0.2

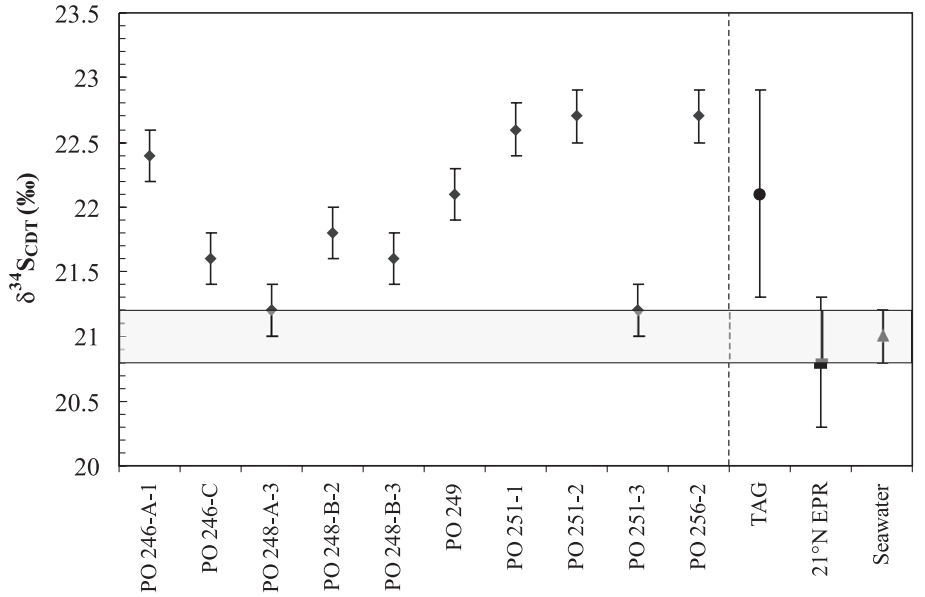

Fig. 4. Results of $\delta^{34}S_{CTD}$ measurements of Grimsey anhydrites compared to literature data (data from Chiba et al., 1998; Haymon and Kastner, 1986). The transparent bar represents seawater values (Rees et al., 1978).

EPR values, but plot close to typical TAG anhydrite (Fig. 4). However, the variance of the Grimsey data is larger than that of TAG or 21°N EPR samples.

Strontium isotopic ratios of anhydrite range from 0.70608 to 0.70732 (ave. = 0.70662) with values from one chimney being rather constant but differ-

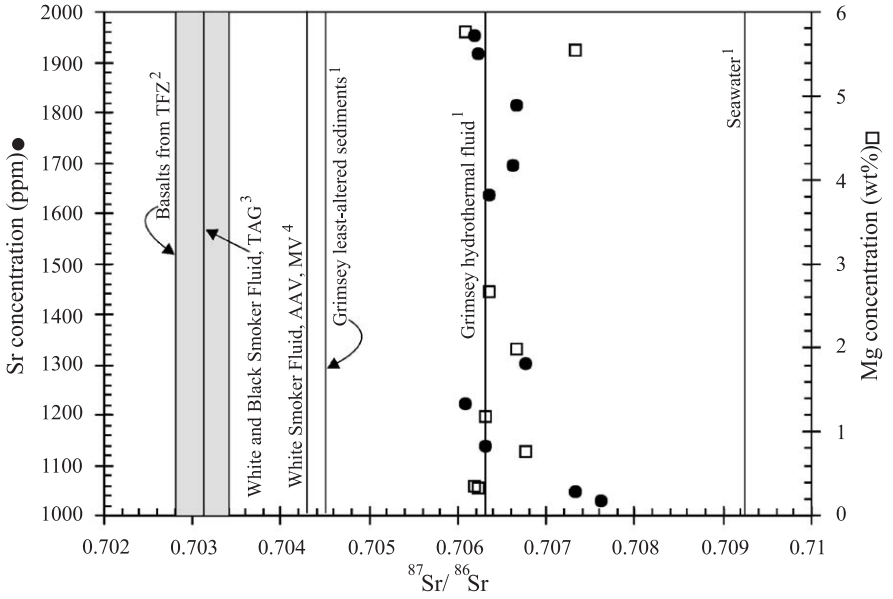

Fig. 5. Results of $^{87}Sr/^{86}Sr$ analyses of Grimsey anhydrites, least-altered sediments and hydrothermal fluids (endmember concentration) compared to literature data, see text for discussion. Data from (1) this study, (2) Schilling et al. (1999), (3) Mills et al. (1998), (4) Butterfield et al. (1994).

ing between chimneys from different sample points (Table 4 and Fig. 5). The Mg-rich sample PO 256-2 has a higher value of 0.70763. The least-altered sediments have a Sr isotopic ratio of 0.70451 which is somewhat elevated compared to basaltic rocks of the TFZ (0.702805–0.703391; Schilling et al., 1999). The endmember $^{87}Sr/^{86}Sr$ of the hydrothermal fluids was calculated on the Mg = 0 basis and is 0.70634 (Fig. 6), the seawater value of this area is 0.709225 which is close to ratios reported from other oceanic regions (Table 2; cf. Teagle et al., 1998a).

In summary, the anhydrite samples have Sr isotopic ratios similar to that of the venting fluids (after reduction of entrained seawater). They generally plot between the sediments/basalts of the Grimsey area which are considered to be the source rocks and seawater (Fig. 5).

3.5. Fluid inclusion studies

Fluid inclusion studies in anhydrite were carried out on two-phase liquid–vapor inclusions in massive anhydrites that homogenize into the liquid phase. They have elongate shapes, 5–25 μm in length and filling grades mainly between 85% and 95%.

Homogenization temperatures (T_H) for all inclusions in anhydrite range from 155 to 289 °C with maxima at about 220 and 240 °C (ave. = 235 °C, $n = 101$; Fig. 7; Table 6). This is consistent with the in situ temperature of the venting fluids determined with the submersible *Jago* (Fig. 2; Table 2).

No phase transitions which point to the existence of CO_2 or other gases were observed during the heating. Therefore, a pure $NaCl–H_2O$ system is suggested for the fluid inclusions which permits the

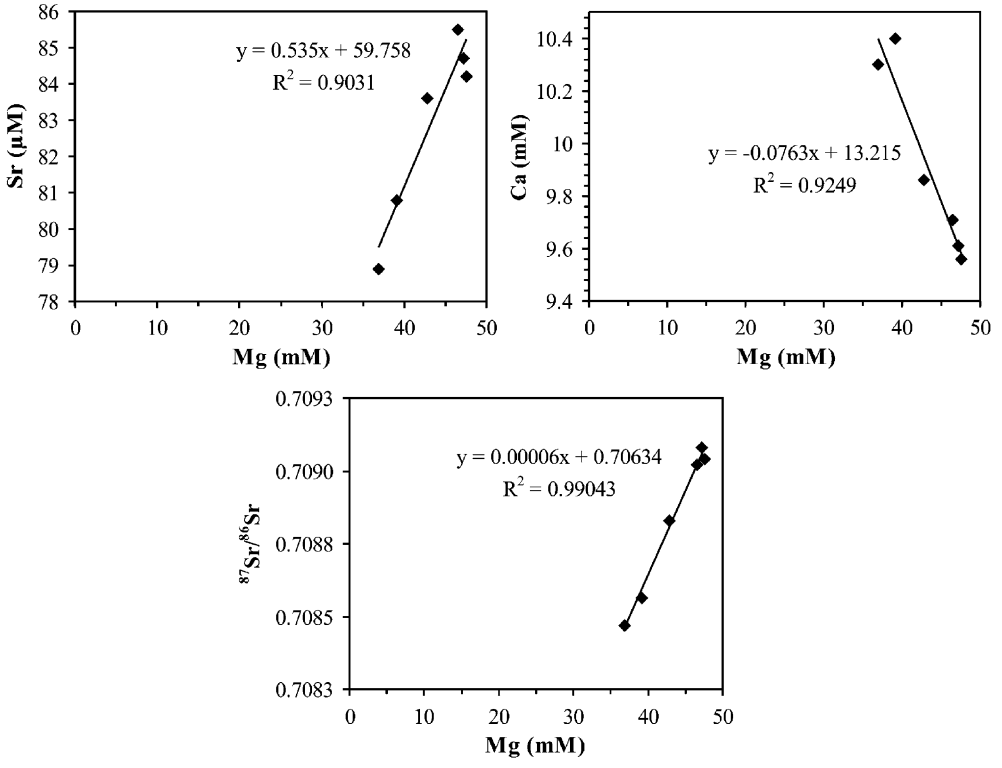

Fig. 6. Calculation of endmember contents of Sr and Ca as well as endmember $^{87}Sr/^{86}Sr$ ratios of the venting fluids based on Mg = 0 normalization.

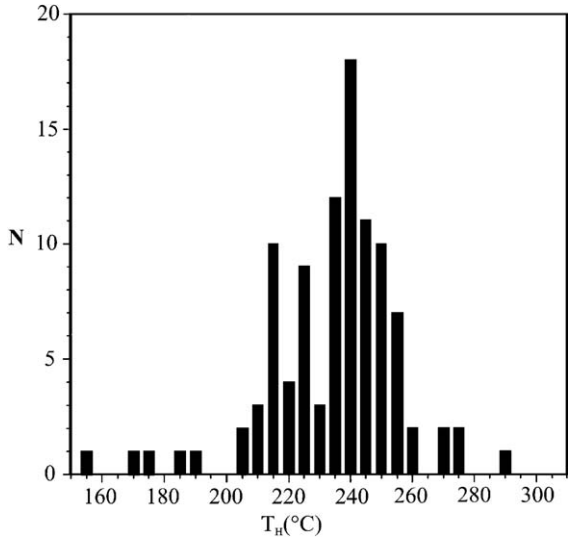

Fig. 7. Frequency diagram of homogenization temperatures of fluid inclusions of anhydrites from the Grimsey hydrothermal field. It is obvious that most of the temperatures range between 200 and 280 °C and therefore, are consistent with the in situ temperature of the venting fluids of 248–250 °C (Stoffers et al., 1997).

calculation of the salinities from the final ice melting temperatures (T_{Melt}; Bodnar, 1993). T_{Melt} values are between −3.4 and −0.6 °C and calculated salinities range from 1.0 to 5.5 wt.% NaCl equivalent averaging 2.5 wt.% NaCl equivalent (n=114; Table 6) or 0.3–1.7 times seawater salinity (average of 3.2 wt.%; Bischoff and Rosenbauer, 1984). The eutectics of all fluid inclusions are between −32 and −18 °C (ave.=−21 °C, n=43) which are close to a pure NaCl–H_2O system (−21.2 °C; Borisenko, 1977).

4. Discussion

In general, seawater which is heated to over 150 °C becomes saturated with respect to $CaSO_4$ and will precipitate anhydrite (Shikazono and Holland, 1983). This may be achieved by (i) conductive heating of seawater by the wallrock or (ii) mixing of seawater with hot hydrothermal fluid. Both processes are recorded in the Sr isotopic ratios and trace element geochemistry (Teagle et al., 1998a).

During mixing of hydrothermal fluids with seawater and precipitation of anhydrite, fractionation of $^{87}Sr/^{86}Sr$ ratios does not occur and $^{87}Sr/^{86}Sr$ ratios in anhydrite represent that of the fluids from which it was precipitated (Mills et al., 1998). Strontium isotopic ratios of anhydrite from the Grimsey field yield values between 0.70608 and 0.70763 (Fig. 5). Some samples contain minor to common amounts of gypsum (Table 3). However, there are no systematic variations of the Sr isotopic data or the geochemical data with the gypsum content. Gypsum may form from anhydrite by the uptake of water, but this should neither change the Sr isotopic systematics, nor the Sr/Ca ratios as long as gypsum does not directly precipitate from seawater. If this were the case, there should be a systematic increase of the Sr isotopic ratios toward the seawater value with higher gypsum contents which is not observed in the samples.

Sample PO 256-2 containing abundant talc-like phases (stevensite–kerolite mixed layer) has only a slightly higher $^{87}Sr/^{86}Sr$ ratio but a distinctly higher partition coefficient (see below) compared to the other samples. The talc-like phases exclusively occur

Table 6
Homogenization temperatures (T_H), final ice melting temperatures (T_{Melt}) and calculated salinities of fluid inclusions in anhydrites from the Grimsey field

Sample	T_H [°C]					T_{Melt} [°C]					Salinity [wt.% NaCl eq.]				
	n	Min	Max	Mean	s	n	Min	Max	Mean	s	n	Min	Max	Mean	s
PO 246 A-1	11	203	253	226	14	11	−1.9	−1.0	−1.6	0.4	11	1.7	3.1	2.6	0.6
PO 246 C	20	188	258	239	15	23	−2.7	−0.7	−1.4	0.5	23	1.2	4.4	2.3	0.8
PO 248 A-3	23	227	277	247	13	24	−2.0	−1.0	−1.5	0.3	24	1.7	3.3	2.5	0.5
PO 249	24	155	268	233	27	26	−2.0	−0.6	−1.0	0.3	26	1.0	3.3	1.7	0.5
PO 251-1	7	226	289	246	21	10	−2.2	−1.4	−1.7	0.3	10	2.3	3.6	2.8	0.4
PO 256-2	16	174	227	212	11	20	−3.4	−1.0	2.0	0.6	20	1.7	5.5	3.3	0.9

n=number of measurements.
s=standard deviation.

in the fluid channelways of the anhydrite chimneys. XRD and chemical analyses indicate that this material is very pure (Kuhn, unpublished data). Even if these results suggest an in situ precipitation of the kerolite–stevensite in the fluid channelways of the anhydrite chimneys, it seems that other processes than pure mixing between hydrothermal fluids and seawater may have played a role during their formation. Therefore, this sample will be excluded from further discussion.

The Sr isotopic ratios of the samples of this study plot close to the endmember value of the venting hydrothermal fluids (Fig. 5). This endmember fluid (Mg = 0) is interpreted to already be a mixture of seawater and a true hydrothermal fluid rising from greater depths beneath the seafloor. This conclusion is supported by (i) the Sr isotopic ratio of the endmember fluid which plots in-between the basalts from the TFZ (including one sample from Grimsey Island: 0.702914; Schilling et al., 1999), the least-altered sediments sampled near the Grimsey field (the deeper hydrothermal fluid should have equilibrated with these source material) and seawater (Fig. 5) as well as (ii) the high SO_4^{2-} content of the endmember fluid (2.72 mmol/l; Garbe-Schönberg unpublished data) which may largely derive from seawater.

The fluid temperatures were measured accurately with a particularly small probe after the chimneys had been knocked over to minimize mixing of the hot fluid with seawater. Most of the measured temperatures were close to 250 °C. This is the maximum temperature possible for hydrothermal fluids at this water depth (400 m) because of the effect of phase separation. Clear evidence of boiling is visible at the venting sites like gas bubbles and the characteristic "flashing". The latter is caused by H_2O vapor (i.e., steam) that condenses rapidly within a few centimeters of the vent orifice (Hannington et al., 2001). Since the venting fluids have maximum possible temperatures, significant mixing of these fluids with cold seawater at the vent sites cannot have taken place. Therefore, the high Mg contents of the sampled fluids (Table 2) is a sampling artefact but does not reflect the composition of the actually venting fluids. The fluids were taken by Niskin bottles with a rather large opening and seawater entrainment is easily possible. This is the reason for the low hydrothermal component of the sampled fluids (Table 2).

Homogenization temperatures measured in the fluid inclusions of anhydrite are close to the in situ measured fluid temperatures (Fig. 7). Strontium isotopic ratios of anhydrite are also similar to the endmember fluid (Fig. 5). These results indicate that anhydrite precipitated from fluids similar to those currently venting in the field (Table 6). Therefore, it is possible to compare Sr/Ca ratios in anhydrite samples and in the corresponding parent fluids. Doerner–Hoskin type models have been established to be an appropriate description of trace element partitioning into crystalline systems during unidirectional precipitation of minerals (Shikazono and Holland, 1983; Mills and Tivey, 1999). Following this approach, the partitioning of trace elements between a solid and a fluid is controlled by the partition coefficient D. In the case of the Sr/Ca system, D can be calculated as follows (Mills and Tivey, 1999):

$$D_{Sr} = \frac{(Sr/Ca)_{solid}}{(Sr/Ca)_{fluid}}$$

with Sr/Ca being molar ratios. For the fluid, the calculated endmember value of 4.53 has been used (Table 2).

The partition coefficients for Grimsey anhydrites range from 0.49 to 0.77 (average: 0.67; Table 4). These values are similar to acicular anhydrite which precipitated from extremely supersaturated solutions in laboratory experiments ($D_{Sr} = 0.52–0.55$; Shikazono and Holland, 1983) and to values reported from other marine hydrothermal systems (ranging from 0.35 to 1.0; Teagle et al., 1998a). They are also similar to anhydrite from the stockwork zone at TAG but considerably lower than surface anhydrite at TAG (Fig. 8; Teagle et al., 1998a; Mills and Tivey, 1999).

The fluid composition is one of the main factors which may influence the partition coefficient (Shikazono and Holland, 1983; Mills and Tivey, 1999). Anhydrites from the central black smoker area at TAG have high D_{Sr}. They precipitated from an evolved fluid which developed during the ascend of a black smoker fluid and continuous mixing with entraining seawater at different depths. In contrast, anhydrites precipitating from white smoker fluids have low D_{Sr} like those from Grimsey. White smoker fluids at TAG form from mixing of a rising hydro-

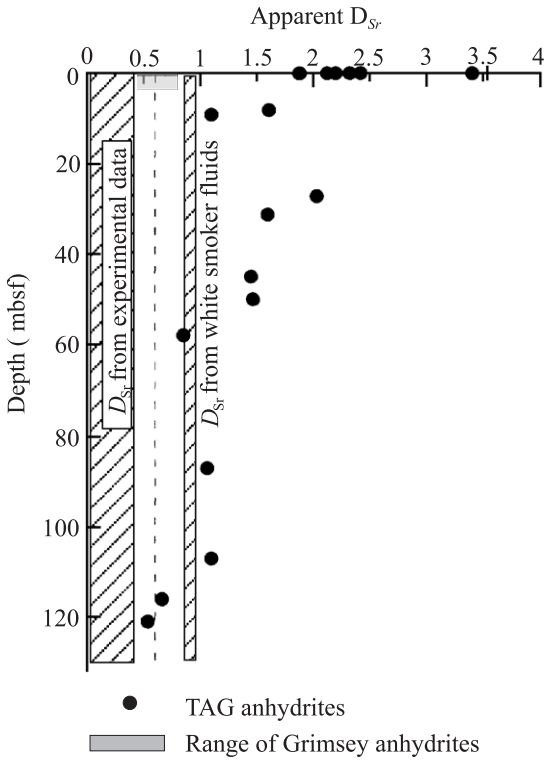

Fig. 8. Apparent D_{Sr} of Grimsey anhydrites compared to downcore variation of D_{Sr} in TAG samples and D_{Sr} from white smoker fluid and experimental data (from Shikazono and Holland, 1983; Mills and Tivey, 1999). Low D_{Sr} at TAG represents precipitation from a fluid which was not evolved; high D_{Sr} corresponds to an evolved fluid (i.e., continued mixing of a rising black smoker fluid with deeply entrained and heated seawater and subsequent anhydrite precipitation). Grimsey anhydrites have low D_{Sr} and are probably similar to D_{Sr} from a white smoker fluid at TAG.

thermal fluid and seawater circulating just beneath the hydrothermal mound (Mills et al., 1998). It is suggested that the situation at the Grimsey hydrothermal field may be similar.

A model for the Grimsey field includes a hydrothermal fluid rising from deep below the seafloor. It may precipitate its metal content somewhere at depth below the seafloor due to boiling (Hannington et al., 2001), the vapor-dominated phase may further rise close to the seafloor (the hydrothermal endmember fluid has a chlorinity of 274 mM which is about half the seawater chlorinity; Garbe-Schönberg unpublished data) where it mixes with entraining seawater before this mixture ascends to the seafloor. The seawater signature of the $\delta^{34}S_{anhydrite}$ data further supports this model. Since the venting fluids have temperatures of around 250 °C, the hydrothermal fluid–seawater mixture and/or the entraining seawater have to be conductively heated which will eventually result in anhydrite precipitation both at and beneath the seafloor (Fig. 9). To what extent this conductive heating takes place can be estimated from the relative proportion of seawater in the mixed fluids.

If equilibration of a black smoker fluid with the sediments at Grimsey is assumed, this fluid should have the same $^{87}Sr/^{86}Sr$ as the sediments (0.704512; Table 4). It is further suggested that about 10% of the Sr content of the sediments is leached by the black smoker fluid resulting in a Sr concentration of 274 μM in the fluid. A similar proportion of Sr was suggested by Teagle et al. (1998b) to be leached from TAG-MORB in equilibrium with black smoker fluids. It is now possible to calculate the relative hydrothermal fluid proportion after mixing with entraining seawater beneath the Grimsey hydrothermal field using formula (1) by Mills et al. (1998):

$$\%\ \text{hydrothermal component} = 100 * \frac{[^{87}Sr/^{86}Sr_{SW} * (Sr)_{SW}] - [^{87}Sr/^{86}Sr_{M} * (Sr)_{SW}]}{[^{87}Sr/^{86}Sr_{SW} * (Sr)_{SW}] - [^{87}Sr/^{86}Sr_{HT} * (Sr)_{HT}] + \{^{87}Sr/^{86}Sr_{M} * [(Sr)_{HT} - (Sr)_{SW}]\}}$$

where subscripts SW, HT and M refer to seawater, hydrothermal fluid and measured fluid values, respectively. For the hydrothermal fluid, the $^{87}Sr/^{86}Sr$ is 0.704512 and the Sr concentration is 274 μM (see above); as measured values, the calculated Sr concentration and Sr isotopic ratios from the Mg = 0 endmember have been used (Fig. 6).

The used values result in a mixture of 37% hydrothermal solution and 63% seawater at shallow depth beneath the mound. Nearly the same propor-

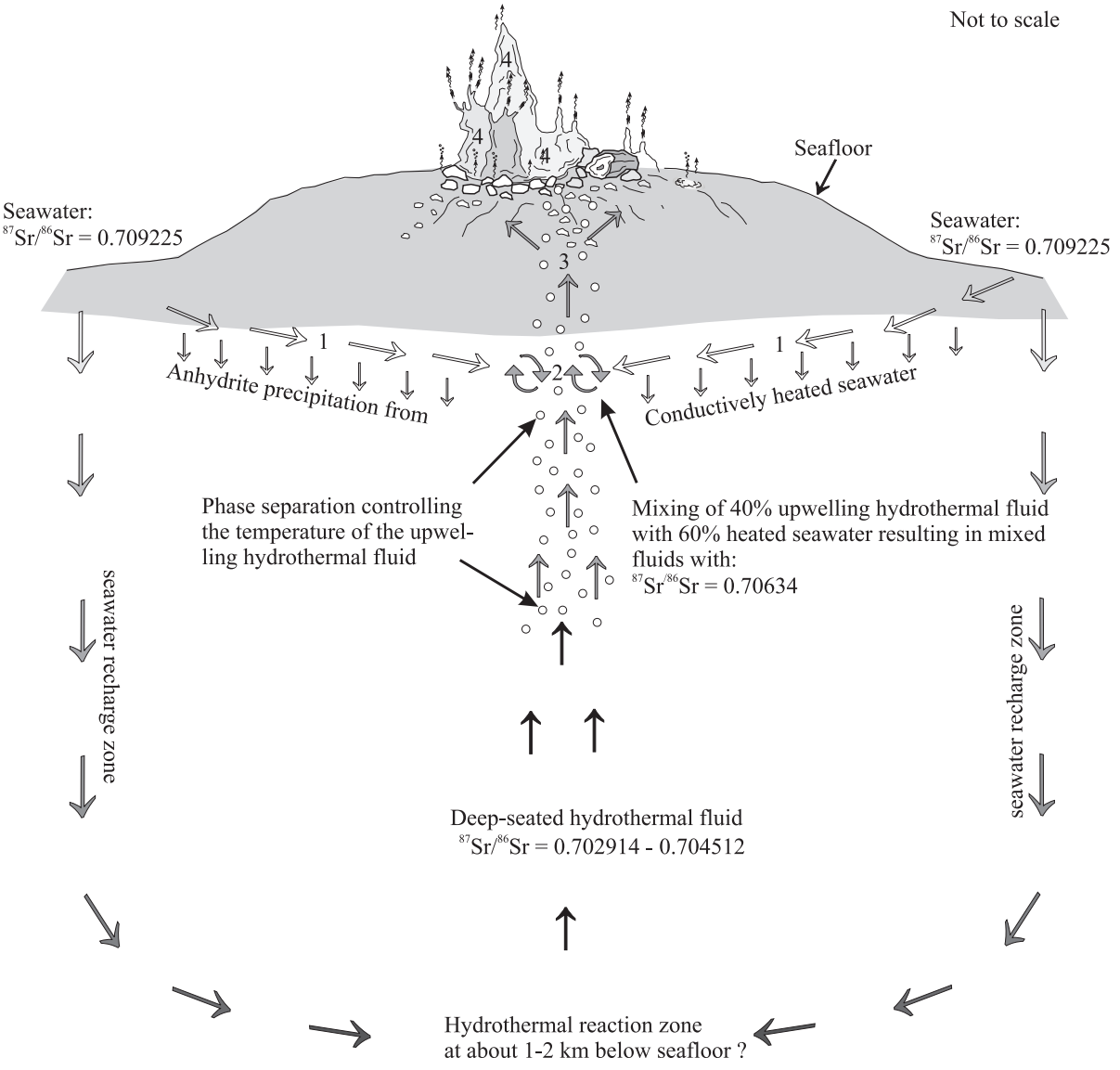

Fig. 9. Schematic drawing showing the main processes related to Sr–Ca geochemistry at Grimsey hydrothermal field. Seawater ($^{87}Sr/^{86}Sr = 0.709225$) entraining the seafloor to shallow depth is heated to >150 °C leading to anhydrite precipitation (1). The heating of seawater is either conductively or caused by mixing with upwelling hydrothermal fluid. It is assumed that the latter has equilibrated with sediment or underlying basalt resulting in $^{87}Sr/^{86}Sr = 0.702914 - 0.704512$ (Schilling et al., 1999). The temperature of the ascending hydrothermal solution is controlled by phase separation and cannot exceed 250 °C at shallow depth. The mixed fluid being further conductively heated to 250 °C has $^{87}Sr/^{86}Sr = 0.70634$ (2). This fluid rapidly rises to the seafloor (3) and precipitates anhydrite at and beneath the seafloor (4).

tions (40%–60%) results if the hydrothermal fluid equilibrates with basalts at depth ($^{87}Sr/^{86}Sr$: 0.702914; Sr: 1220 μM at Grimsey Island; Schilling et al., 1999). Theses estimates suggest that a large amount of cold seawater entrains to shallow depth and is conductively heated to more than 200 °C which requires a large and continuous heat flow in the Grimsey hydrothermal field. This conclusion is consistent with very high temperature gradients measured in the sediments during a recent R/V *Poseidon* cruise to the Grimsey field (52.34–61.27 °C/m; Devey and shipboard scientific party, 2002).

Subcritical phase separation (boiling) in the Grimsey field may also have an influence on the Sr/Ca ratio of the hydrothermal fluid. Data from other boiling seafloor hydrothermal systems show that Sr/Ca ratios differ between the brine- and vapor-dominated phase (i.e., at North Cleft segment, Juan de Fuca Ridge: Sr/Ca_{Brine}:2.94–3.19, Sr/Ca_{Vapor}: 4.92; Butterfield and Massoth, 1994). Therefore, boiling may account for the differences of the molar Sr/Ca ratio of the Grimsey hydrothermal fluid endmember (4.53 mmol/mol) compared to white smoker fluids at TAG (2.62 mmol/mol; Mills et al., 1998). Reducing the molar Sr/Ca of the venting fluids from 4.53 to 2.6 (taking into account a difference of 1.9 between the brine- and vapor-dominated phases), the recalculated D_{Sr} would be between 0.86 and 1.34 (ave. 1.17). This is a slight shift toward higher D_{Sr} values. Nevertheless, the partition coefficients of Grimsey anhydrites remain considerably smaller than those of surface anhydrites from TAG. Therefore, even if boiling is responsible for a shift in the molar Sr/Ca ratio of the venting fluid at Grimsey to higher values, the principal result of this study, that is, anhydrite precipitation from non-evolved fluids, does not change.

5. Conclusions

Anhydrite occurring as chimneys and crusts at the seafloor of the Grimsey hydrothermal field has formed by precipitation from a mixture of hydrothermal fluid and seawater. In contrast to the black smoker area at TAG, seawater entrains only to shallow depth and no continuous fluid evolution takes place. Molar Sr/Ca data of both the fluids and the precipitates as well as the temperature of the emanating fluids suggest that at least part of the dissolved Ca-sulfate is precipitated either before or during mixing. Therefore, an anhydrite-rich zone should be present beneath the Grimsey hydrothermal field.

This study shows that Sr isotopic data and Sr/Ca systematics of surface anhydrite and fluid samples can provide information for the fluid evolution at depth.

Acknowledgements

Thanks are due to the staff of the geochemical and mineralogical laboratories at Freiberg University of Mining and Technology, the Geological Survey of Canada in Ottawa and the University of Kiel. We wish to express our appreciation to the captains and crew of R/V *Poseidon* and especially to Jürgen Schauer and Karen Hissmann for operating the submersible *Jago*. Cornelia Stegmann is acknowledged for providing unpublished data of her MSc thesis. This paper largely benefited from the comments of R.A. Mills and P. Anschutz. Our research was supported through grant He-1660/10 and the Leibniz Program of the German Research Foundation (DFG). **[RR]**

References

Ames, D.E., Franklin, J.M., Hannington, M.D., 1993. Mineralogy and geochemistry of active and inactive chimneys and massive sulfides, Middle Valley, Northern Juan de Fuca Ridge: an evolving hydrothermal system. Can. Mineral. 31, 997–1024.

Benjaminsson, J., 1988. Jardhiti i sjo og flaedamali vid Island (Geotherma activity in the tidal zone and below sea level around Iceland, English abstract). Natturufraedingurinn 58, 153–169.

Bischoff, J.L., Rosenbauer, R.J., 1984. The critical point and two-phase boundary of seawater, 200–500 °C. Earth Planet. Sci. Lett. 68, 172–180.

Bischoff, J.L., Seyfried, W.E., 1978. Hydrothermal chemistry of seawater from 25 °C to 350 °C. Am. J. Sci. 278, 838–860.

Bodnar, R.J., 1993. Revised equation and table for determining the freezing point depression of H_2O–NaCl solutions. Geochim. Cosmochim. Acta 57, 683–684.

Borisenko, A.S., 1977. Study of the salt composition of solutions in gas–liquid inclusions in minerals by the cryometric methods. Sov. Geol. Geophys. 18, 11–19.

Butterfield, D.A., Massoth, G.J., 1994. Geochemistry of North Cleft segment vent fluids: temporal changes in chlorinity and

their possible relation to recent volcanism. J. Geophys. Res. 99 (B3), 4951–4968.

Butterfield, D.A., McDuff, R.E., Franklin, J., Wheat, C.G., 1994. Geochemistry of hydrothermal vent fluids from Middle Valley, Juan de Fuca Ridge. In: Mottl, M.J., Davis, E.E., Fisher, A.T., Slack, J.F. (Eds.), Proc. Ocean Drill. Program, Sci. Results, vol. 139, pp. 395–410. College Station, TX.

Chiba, H., Uchiyama, N., Teagle, D.A.H., 1998. Stable isotope study of anhydrite and sulfide minerals at the TAG hydrothermal mound, Mid-Atlantic Ridge, 26°N. In: Herzig, P.M., Humphris, S.E., Miller, D.J., Zierenberg, R.A. (Eds.), Proc. Ocean Drill. Program, Sci. Results, vol. 158, pp. 85–90. College Station, TX.

Devey, C.W., shipboard scientific party, 2002. Hydrothermal studies of Grimsey Field, volcanic studies of Kolbeinsey Ridge. Cruise Report POS 291 of R/V Poseidon, University of Bremen. 42 pp.

Devey, C.W., Wieneke, M., Haase, K.M., 1997. High-density sampling of the Kolbeinsey Ridge: details of the magmatic chemistry of a slow-spreading axis. International Ridge-Crest Research: 4D Architecture 6, 2.

Fricke, H., Giere, O., Stetter, K., Alfredsson, G.A., Kristjansson, J.K., Stoffers, P., Svarvasson, J., 1989. Hydrothermal vent communities at the shallow subpolar Mid-Atlantic ridge. Mar. Biol. 102, 429–435.

German, C.R., Briem, J., Chin, C., Danielson, M., Holand, S., James, R., Jonsdottir, A., Ludford, E., Moser, C., Olafsson, J., Palmer, M., Rudnicki, M.D., 1994. Hydrothermal activity on the Reykjanes Ridge: the Steinaholl vent field at 63°06′ N. Earth Planet. Sci. Lett. 121, 647–654.

Goodfellow, W.D., Grapes, K., Cameron, B., Franklin, J.M., 1993. Hydrothermal alteration associated with massive sulfide deposits, Middle Valley Northern Juan de Fuca Ridge. Canadian Mineralogist 31, 1025–1060.

Goodfellow, W.D., Zierenberg, R.A., 1999. Genesis of massive sulfide deposits at sediment-covered spreading centres. In: Barrie, C.T., Hannington, M.D. (Eds.), Volcanic-Associated Massive Sulfide Deposits: Processes and Examples in Modern and Ancient Settings. Rev. Econ. Geol., vol. 8. SEG, Littleton, CO, pp. 297–324.

Hannington, M., Herzig, P., Stoffers, P., Scholten, J., Garbe-Schönberg, D., Jonasson, I.R., Roest, W., 2001. First observations of high-temperature submarine vents and massive anhydrite deposits off the north coast of Iceland. Mar. Geol. 177, 199–220.

Haymon, R.M., Kastner, M., 1981. Hot spring deposits on the East Pacific Rise at 21°N: Preliminary description of mineralogy and genesis. Earth Planet. Sci. Lett. 53, 363–381.

Haymon, R.M., Kastner, M., 1986. The formation of high temperature clay minerals from basalt alteration during hydrothermal discharge on the East Pacific rise axis at 21°N. Geochim. Cosmochim. Acta 50, 1933–1939.

Heinrichs, H., Herrmann, A.G., 1990. Praktikum der Analytischen Geochemie. Springer-Verlag, Berlin. 669 pp.

Mills, R.A., Tivey, M.K., 1999. Sea water entrainment and fluid evolution within the TAG hydrothermal mound: evidence from analyses of anhydrite. In: Cann, J.R., Elderfield, H., Laughton, A. (Eds.), Mid-Ocean Ridges. The Royal Society, Cambridge, pp. 225–263.

Mills, R.A., Teagle, D.A.H., Tivey, M.K., 1998. Fluid mixing and anhydrite precipitation within the TAG mound. In: Herzig, P.M., Humphris, S.E., Miller, D.J., Zierenberg, R.A. (Eds.), Proc. Ocean Drill. Program, Sci. Results, vol. 158, pp. 119–127. College Station, TX.

Olafsson, J., Honjo, S., Thors, K., Stefansson, U., Jones, R.R., Ballard, R.D., 1989. Initial observation, bathymetry and photography of a geothermal site on the Kolbeinsey Ridge. In: Ayala-Castanares, A., Wooster, W., Yanez-Arancibia, A. (Eds.), Oceanography 1988. UNAM Press, Mexico, pp. 121–127.

Rees, C.E., Jenkins, W.J., Monster, J., 1978. The sulphur isotopic composition of ocean water sulphate. Geochim. Cosmochim. Acta 42, 377–381.

Rögnvaldsson, S., Gudmundsson, A., Slunga, R., 1998. Seismotectonic analysis of the Tjörnes Fracture Zone, an active transform fault in north Iceland. J. Geophys. Res. 103, 30117–30129.

Schilling, J.-G., Kingsley, R., Fontignie, D., Poreda, R., Xue, S., 1999. Dispersion of the Jan Mayen and Iceland mantle plumes in the Arctic: a He-Pb-Nd-Sr isotope tracer study of basalts from the Kolbeinsey, Mohns, and Knipovich Ridges. J. Geophys. Res. 104 (B5), 10543–10569.

Scholten, J., Blaschek, H., Becker, K.-P., Hannington, M., Herzig, P., Hißmann, K., Jonasson, I., Krüger, O., Marteinsson, V., Preißler, H., Schauer, J., Schmidt, M., Solveig, P., Theißen, O., 2000. Hydrothermalism at the Kolbeinsey Ridge, Iceland. Technical Cruise Report PO 253, University of Kiel, pp. 22–43.

Shannon, R.D., 1976. Revised effective ionic radii and systematic studies of interatomic distances in halides and chalcogenides. Acta Crystallogr. (32), 751–767.

Shikazono, N., Holland, H.D., 1983. The partitioning of strontium between anhydrite and aqueous solutions from 150° to 250°C. Econ. Geol. Monogr. 5, 320–328.

Shikazono, N., Holland, H.D., Quirk, R.F., 1983. Anhydrite in Kuroko deposits: mode of occurrence and depositional mechanisms. Econ. Geol. Monogr. 5, 329–344.

Stegmann, S., 1998. Mineralogische und geochemische Untersuchungen von hydrothermalen Präzipitaten des Kolbeinsey Rückens vor Island. Unpublished MSc thesis, TU Bergakademie, Freiberg. 125 pp.

Stoffers, P., Botz, R., Garbe-Schönberg, D., Hannington, M., Hauzel, B., Herzig, P., Hissmann, K., Huber, R., Kristjansson, J.K., Petursdottir, S.K., Schauer, J., Schmitt, M., Zimmerer, M., 1997. Cruise Report Poseidon 229 "Kolbeinsey Ridge", University of Kiel. 58 pp.

Teagle, D.A.H., Alt, J.C., Chiba, H., Halliday, A.N., 1998a. Dissecting an active hydrothermal deposit: the strontium and oxygen isotopic anatomy of the TAG hydrothermal mound-anhydrite. In: Herzig, P.M., Humphris, S.E., Miller, D.J., Zierenberg, R.A. (Eds.), Proc. Ocean Drill. Program, Sci. Results, vol. 158, pp. 129–141. College Station, TX.

Teagle, D.A.H., Alt, J.C., Chiba, H., Humphris, S.E., Halliday, A.N., 1998b. Strontium and oxygen isotopic constraints on fluid

mixing, alteration and mineralization in the TAG hydrothermal deposit. Chem. Geol. 149, 1–24.

Tichomirowa, M., Berger, H.-J., Koch, E.A., Belyatski, B.V., Götze, J., Kempe, U., Nasdala, L., Schaltegger, U., 2001. Zircon ages of high-grade gneisses in the Eastern Erzgebirge (Central European Variscides)—constraints on origin of the rocks and Precambrian to Ordovician magmatic events in the Variscan foldbelt. Lithos 56, 303–332.

Ueda, A., Krouse, H.R., 1986. Direct conversion of sulphide and sulfate minerals to SO_2 for isotope analyses. Geochem. J. 20, 209–212.